Catalysis Today 432 (2024) 114615

Contents lists available at ScienceDirect

Catalysis Today

journal homepage: www.elsevier.com/locate/cattod

Rational process design for the efficient oxidation of crude HMF-solution using AuPd/C catalysts

Dominik Neukum [a], Erisa Saraçi [a,b,*], Dominik Wüst [c], Ajai Raj Lakshmi Nilayam [d,e], Shweta Sharma [b], Jan-Dierk Grunwaldt [a,b,*]

[a] Institute of Catalysis Research and Technology, Karlsruhe Institute of Technology, Hermann-von-Helmholtz-Platz 1, Eggenstein-Leopoldshafen 76344, Germany
[b] Institute for Chemical Technology and Polymer Chemistry, Karlsruhe Institute of Technology, Engesserstraße 20, Karlsruhe 76131, Germany
[c] Institute of Agricultural Engineering, University of Hohenheim, Garbenstraße 9, Stuttgart 70593, Germany
[d] Institute of Nanotechnology, Karlsruhe Institute of Technology, Hermann-von-Helmholtz-Platz 1, Eggenstein-Leopoldshafen 76344, Germany
[e] Karlsruhe Nano Micro Facility (KNMFi), Karlsruhe Institute of Technology, Hermann-von-Helmholtz-Platz 1, Eggenstein-Leopoldshafen 76344, Germany

ARTICLE INFO

Keywords:
Oxidation
HMF
Sustainable chemistry
Heterogeneous catalysis
Noble metal
Bio-based

ABSTRACT

The oxidation of 5-(Hydroxymethyl)furfural (HMF) to 2,5-furandicarboxylic acid (FDCA) is of high interest for the production of renewable monomers. To achieve a cost-efficient, sustainable process for the large-scale production of FDCA, it is important to use the as-synthesized crude HMF-solution without extensive purification steps. In this work, we present the direct oxidation of crude HMF-solution produced from fructose syrup with an AuPd/C catalyst. The catalyst shows good tolerance against various remaining impurities from the HMF-preparation. A 95% FDCA yield with a productivity of 75.5 mol_{FDCA} mol_{AuPd}^{-1} h^{-1} could be achieved under increased temperature (140 °C) and pressure (40 bar) with only 2 eq. Na_2CO_3. We further improved the process' efficiency by using a two-step oxidation with a split addition of the base in the same reactor. First, a mild oxidation (1 eq. Na_2CO_3, 100 °C, 1.5 h) of HMF afforded the intermediates HFCA and FFCA, which were then further oxidized under harsher conditions (3.3 eq. NaOH, 140 °C, 4 h) to FDCA. Due to the higher efficiency, this process enabled increasing the HMF concentration up to 0.3 M for crude solution and 0.6 M for purified solution while minimizing the degradation of HMF, leading to a more cost-efficient oxidation of crude HMF-solution, and facilitating the industrial implementation of renewable FDCA.

1. Introduction

Reducing the reliance on fossil resources within the chemical industry has become an important aspect of research in recent years.[1] Establishing, a circular-economy with a short carbon cycle is crucial to achieve this goal, including the substitution of fossil-derived base--chemicals by renewable alternatives.[2,3] Bio-based chemicals can play an important role towards a CO_2-neutral chemical industry, leading to a significant reduction in greenhouse gas emissions.[4] One important bio-based platform molecule is 5-(Hydroxymethyl)furfural (HMF), which can be transformed to various different products.[5] The oxidation of HMF to 2,5-Furandicarboxylic acid (FDCA) offers the opportunity to produce a bio-based monomer poised to replace terephthalic acid in renewable polyesters.[6,7] Numerous catalytic and stoichiometric routes for HMF oxidation have been reported in literature.[8–12] Heterogeneously catalyzed processes offer a distinct advantage - an easy separation of the catalyst from the reaction mixture, facilitating the reusability of the catalyst. These catalysts often feature noble metals (such as Au, Pd, Pt, Ru) supported on metal oxides or carbon-based materials.[8,13]

Current research on HMF-oxidation has mainly focused on the use of highly purified and diluted HMF-solutions in batch processes at small scale. There is a significant gap in experimentation involving crude HMF-solution produced directly from biomass or saccharides, without extensive and costly purification. Economic simulations on the heterogeneously catalyzed oxidation of HMF showed that the HMF price and the catalyst cost are the two major contributions to the FDCA cost.[14] Therefore, applying crude HMF solution directly in the oxidation process eliminates the need for costly purification and crystallization steps associated with the production of purified HMF, thereby enhancing the

* Corresponding authors at: Institute of Catalysis Research and Technology, Karlsruhe Institute of Technology, Hermann-von-Helmholtz-Platz 1, Eggenstein-Leopoldshafen 76344, Germany.
E-mail addresses: erisa.saraci@kit.edu (E. Saraçi), grunwaldt@kit.edu (J.-D. Grunwaldt).

https://doi.org/10.1016/j.cattod.2024.114615
Received 20 December 2023; Received in revised form 23 February 2024; Accepted 27 February 2024
Available online 28 February 2024

overall process cost-efficiency.[15] To further optimize the cost, it is crucial to use a tolerant catalyst suitable for converting crude HMF, which enables the efficient use of minimal catalyst amounts.[13]

Earlier studies by Naim and Schade et al.[16] have underscored the detrimental impact of impurities arising from the HMF-synthesis on noble metal-based heterogeneous catalysts for HMF oxidation. A mixture of levulinic and formic acid, common by-products from HMF-synthesis, led to severe deactivation of an Au/ZrO_2 catalyst.[16] The FDCA yield dropped from 100% to 0% while HMF conversion simultaneously declined from 100% to 56%. When applying harsher conditions (125 °C, 30 bar air, 8 eq. NaOH) monosaccharides could be tolerated, resulting in a remarkable FDCA yield of $\geq$ 94%. In addition, it was reported that cysteine, cystine, and arginine dissolved during the extraction of saccharides from chicory roots, used for the HMF-synthesis, can lead to a deactivation of noble metals used for the HMF-oxidation.[17] In that study, AuPd-alloys demonstrated the best stability. Zuo et al.[18] studied the oxidation of a crude HMF-solution produced by Archer Daniels Midland (ADM)[19] from a hexose syrup, which contained impurities like HMF dimer, 2-Hydroxyacetylfuran, and levulinic acid. A 4 wt% HMF-solution was efficiently oxidized to FDCA with a 90% yield using the AMOCO oxidation process. Naim and Schade et al.[16] oxidized crude HMF produced from a non-concentrated sugar syrup over an Au/ZrO_2 catalyst, achieving an FDCA yield of 74%. Additionally, several two-step processes have been reported for the preparation of FDCA from biomass.[15,20–24] FDCA was produced from fructose in a single reactor employing a bi-functional Pd/CC catalyst giving a 85% FDCA yield in the second step and an overall yield of 64%.[25] Gupta et al. demonstrated the direct conversion of fructose to HMF and the further oxidation of the crude solution to FDCA using a $Ni_{0.9}Pd_{0.1}$ catalyst for both reactions in one-pot, achieving 22% FDCA selectivity.[26]

This study delves into employing crude HMF-solution for the HMF oxidation process, with emphasis on assessing the FDCA yield and productivity. The aims include evaluating the feasibility of increasing HMF-concentration and reducing the catalyst mass. These aspects will enable the price a reduction and streamline the up-scaling of FDCA-production. For this study, we used AuPd-alloys supported on carbon black Vulcan® XC72 and synthetic air in the oxidation process. We focused on the influence of temperature, pressure, and the added base equivalents on the FDCA yield. Moreover, we developed a two-step oxidation process characterized by a progressive two-step increase in basicity. This approach enables the utilization of higher concentrations of HMF-solution in a single reactor while suppressing side-reactions effectively.

2. Experimental

2.1. Catalyst preparation

52:48 (molar ratio) AuPd was prepared using a slightly modified synthesis protocol reported earlier by our group.[17] $PdCl_2$ (m = 0.0222 g) and $HAuCl_4 \bullet 3\ H_2O$ (m = 0.0533 mg) were dissolved in 3 mL conc. HCl and 77 mL H_2O by stirring for about 3 h. 620 mL of H_2O and poly(vinylalcohol) (PVA; m(Au+Pd):m(PVA) = 1:0.95; m = 37.8 mg) were added to the solution. After about 10 min of stirring a diluted $NaBH_4$ solution (n($NaBH_4$):n(Au+Pd) = 4:1; m = 39.4 mg) was added. The suspension was stirred for about 30 min before adjusting the pH to 1 with 50 vol% H_2SO_4 solution. Then carbon black Vulcan® XC72 (m = 1.96 g) was added to the suspension to achieve a AuPd-loading of 2 wt%, stirred for about 2 h and filtered off. The supported catalyst was washed thoroughly with about 400 mL of H_2O and dried at 80 °C overnight. More details on the chemicals and materials used can be found in the supporting information.

2.2. Catalyst characterization

For elemental analysis, the catalysts were dissolved in a mixture of 6 mL H_2O_2, 2 mL conc. HNO_3 and 4 mL conc. HCl under microwave irradiation of 600 W for 90 min prior to the determination of the metal loading by inductively coupled plasma-optical emission spectrometry (ICP-OES, Agilent 725 spectrometer, Agilent Technologies Inc.). A plasma excitation of 40 MHz and 2 kW was used.

Powder X-ray diffraction (XRD) was performed with a PANalytical X'pert Pro diffractometer using Cu-K_α radiation and a Ni-Filter. Data were recorded with a step size of 0.017 ° in a 2θ-range from 5 to 120 ° by averaging 8 scans. The crystallite size was estimated by fitting the data with Origin2019 and applying the Scherrer equation (cf. ESI).[27] LaB_6 was used as reference.

Scanning transmission electron microscopy (STEM; ThermoFisher Themis 300 (S)TEM) was performed with a high-angle annular dark-field (HAADF) detector to obtain images of the supported nanoparticles. Energy dispersive X-ray (EDX) spectroscopy was conducted with a ThermoFisher Scientific Super-X EDX detector. Standard Lacey carbon grid with Cu mesh was used for sample preparation. Agglomerated particles were not considered in the particle size distribution.

X-ray absorption spectroscopy (XAS) was performed for determination of the oxidation state and estimation of the homogeneity of alloying. AuPd/C, Au-foil, Pd-foil and PdO references were measured at P65 beamline at PETRA III (Deutsches Elektronen Synchrotron, Hamburg).[28] The measurements were performed at Pd K-edge (24.35 keV) and Au L_3-edge (11.919 keV) in transmission mode using ionization chambers and an 11 period undulator. A pair of plane mirrors (Pt-coated Si for Pd K-edge, Si for Au L_3-edge) rejected higher harmonics and the energy was selected with a double-crystal monochromator with Si(311) or Si (111) crystal pairs with a beam size of 1.2 ×0.3 mm. The powder catalyst was filled densely in a 6 mm diameter plastic tube. Athena and Artemis from the Demeter software package (version 0.9.26) were used for data analysis.[29] For data reduction and extraction of the extended X-ray absorption fine structure (EXAFS) part (χ(k) function), a Rbkg value of 1 was considered. For fitting of the EXAFS part of the spectra, a k range of 3–12 $Å^{-1}$ and an R value of 1.5–3.5 Å were taken into account. The amplitude reduction factors (S_0^2) were obtained by fitting the respective foil references.

2.3. HMF preparation

The HMF production was performed by hydrothermal dehydration of an aqueous solution of 2 wt% fructose at Hohenheim's Biorefinery Research Center at "Unterer Lindenhof". Details on the HMF-synthesis procedure were reported recently by Świątek *et al.*[30] Sulfuric acid was used as a catalyst at a pH of 2. For the synthesis, 180 °C, a pressure of 24 bar inside the reactor and a residence time of 18 min were applied. The fructose solution was pumped with a piston pump after reaching the set temperature in the reactor. Afterwards, the solution is cooled down to room temperature in a cooler. Solid residues were removed by a mesh filter. Fructose conversion was 47.2%, HMF selectivity was 71.5%, and HMF yield was 33.6%. Following the HMF synthesis, HMF was separated from the reaction mixture, using Hohenheim's novel separation procedure.[31] In brief, HMF is adsorbed on activated carbon from the aqueous reaction solution. Then, HMF is desorbed from activated carbon applying ethanol as solvent. 90–95% HMF could be recovered from the activated carbon. After the separation process, ethanol was removed by distillation and the crude HMF was dissolved in water. No residual ethanol could be determined in HPLC analysis.

2.4. HMF oxidation procedure

The crude HMF solution was diluted with H_2O to the corresponding concentration (0.1–0.3 M). A sample (diluted 1:50) was taken prior to each experiment to determine the HMF concentration via HPLC analysis. The solution (8 mL) was filled in a poly(tetrafluoroethylene) (PTFE) inset (50 mL volume) in an autoclave reactor. Next, the AuPd/C catalyst (28.8–172.8 mg) and the base (169.8–635.9 mg Na_2CO_3 or 256.0 mg

NaOH) were added to the solution. The autoclave was purged with synthetic air three times, and pressurized at the specified air pressure (10–50 bar). The reactor was heated to the reaction temperature (70–150 °C). The time when reaching the aimed reaction temperature was taken as starting point for the reaction time. After the reaction (1–6 h), the autoclaves were rapidly cooled down in an ice bath, depressurized and opened. A second sample was taken for determination of the conversion, HFCA/FFCA/FDCA-yields and the C-balance. For calculation of the C-balance, HMF and its oxidation products HFCA, FFCA, and FDCA were taken into account.

For the two-step process, the reaction was initiated as described previously. After the reaction time of the first step was completed (0–2 h), the autoclave was cooled rapidly in an ice bath to about 40 °C. Then, it was depressurized, and opened briefly to add the base for the second step (1017 mg Na_2CO_3 or 192.0–480.0 mg NaOH). Afterwards, the autoclave was closed again, purged three times with synthetic air, and pressurized at 50 bar. The autoclave was heated to a reaction temperature of 140 °C, and the time (1–4 h) for the second reaction step was started after reaching the set temperature. Afterwards, it was continued as described for the one-step reaction.

High-performance liquid chromatography (HPLC) was used for determination of the concentration of the different compounds using a column of type Aminex HPX-87 H (BioRad Laboratories Inc.) and a UV–VIS detector. The eluent was 4 mM H_2SO_4. The measurements were performed at 25 °C and a flow rate of 0.65 mL min^{-1}. Additional information can be found in the supporting information.

Additional information on materials and characterization methods can be found in the supporting information.

3. Results and Discussion

3.1. Catalyst characterization

The ICP-OES elemental analysis of the catalyst showed an Au-loading of 0.9 ± 0.1 wt% and a Pd-loading of 0.6 ± 0.1 wt%. This corresponds to a 45:55 (Au:Pd) molar ratio, which is close to the intended ratio of 52:48. The AuPd particles had a mean particle diameter of 4.5 ± 1.6 nm as determined by STEM (Fig. 1(a),(b)). EDX mapping of the catalyst showed a homogeneous distribution of Au and Pd in the particles indicating the formation of a homogeneous alloy (Fig. 1(c)). The EDX spectrometry of the particle gave a molar Au:Pd ratio of 55:45 (± 3%), which deviates slightly from the ICP-OES result.

XRD was used to confirm the alloy formation and composition of the AuPd-nanoparticles within the AuPd/C catalyst. Besides broad reflections of graphite, distinct reflections of a fcc-phase were observed at a 2θ value of 39.02 ° (Fig. 2(a)). The reflections of metallic Au and metallic Pd are expected at 38.2 ° (ICSD collection code: 64701) and 40.1 ° (ICSD collection code: 648676), respectively. Due to the different atomic sizes of Au and Pd, the incorporation of Au into the Pd lattice results in a lattice expansion. The variation of the lattice parameter exhibits a linear correlation with the mixing ratio, causing the reflection position to shift linearly.[32,33] A 1:1 AuPd alloy would yield a reflection at 39.15 ° 2θ. The observed deviation to 39.02 ° in the reflection fitting of the AuPd/C catalyst aligns with a mixing ratio of 57:43 (Au:Pd), suggesting a slight enrichment of Au in the particle core. The fitted curve of the 39.02 ° reflection was used to estimate the nanoparticles' crystallite size by using the FWHM in the Scherrer equation, yielding a crystallite size of 4.8 (± 0.3) nm.

To further validate the presence of an alloyed phase, XAS measurements of AuPd/C at the Au L_3-edge and Pd K-edge were performed (Figures S1-S5 and Table S1). The X-ray absorption near-edge structure (XANES) of both Au and Pd were similar to the metallic foils but with slight variations typical of alloyed AuPd particles (Figure S1 (a) and (b)). [17] The Fourier transformed extended X-ray absorption fine structure (EXAFS) spectra (Fig. 2(b)), revealed two peaks at a radial distance of 2.2 and 2.9 Å for the Au L_3-edge (not corrected for the phase shift), and 1.9 and 2.8 Å for the Pd K-edge. Interference of Au-Au and Au-Pd backscattering leads to a splitting of the respective peaks, providing direct evidence of alloying.[34,35] In addition, data fitting of the EXAFS-spectrum measured at Au L_3-edge confirmed scattering of Au-Au and Au-Pd in the first shell.[29] A radial distance of 2.8 Å (Table S1) obtained in the fitting aligns with expected literature values for Au-Pd. [17,35,36] The coordination numbers (CN) from fitting are 3.7 ± 0.4 for Au-Pd and 7.6 ± 0.7 for Au-Au, with a total CN of 11.3, close to the CN of 12 in the bulk fcc-structure. Hence, the contribution of surface Au-atoms is rather low. The ratio of the CNs of Au-Pd to Au-Au deviates with 2:1 from the ratio found by ICP-OES, which is close to 1:1. Combining both observations from the fitting, suggests potential enrichment of Pd towards the surface while Au might be concentrated in the particle core. [37]

3.2. Crude HMF-solution evaluation

The HMF was synthesized by hydrothermal dehydration of fructose syrup.[30] The HMF synthesis produces a solution that may contain other impurities along with HMF.[16,17] The chemical analysis of the crude, concentrated HMF-solution used in this work is given in Table 1. Notably, it contained 660 g L^{-1} HMF, which corresponds to about 5.2 M. The HMF-solution was diluted to the specified concentration prior to the oxidation reaction. However, the initially high concentration provided an opportunity to explore higher starting concentrations than those typically reported in literature. This approach aimed to reveal the maximum feasible HMF-concentration for the oxidation of both crude and purified solutions. In reported studies involving pure HMF-solutions, the concentration of HMF typically ranged from 0.02 to 0.15 M.[38–45] Higher concentrations in previous studies could only be achieved by complex multi-step processes, including the protection of the aldehyde function of HMF with an additional auxiliary, and the

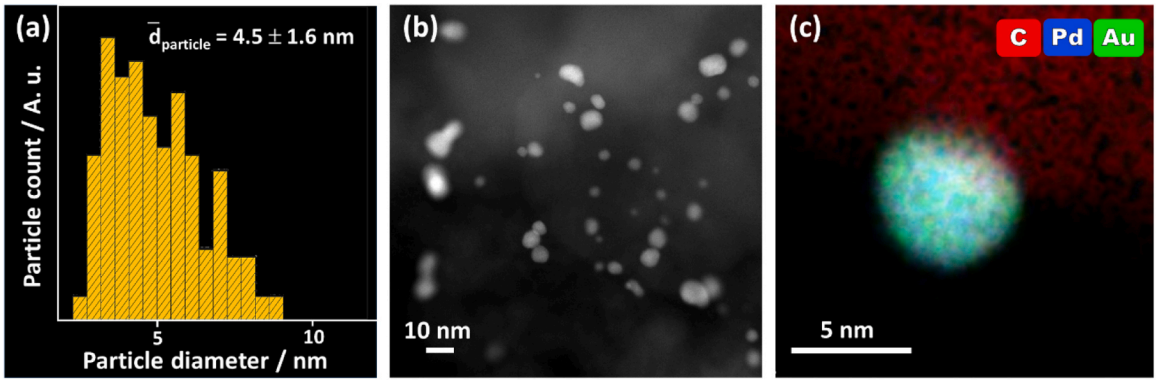

Fig. 1. (a) Particle size distribution (particle count: 273), (b) HAADF-STEM image, and (c) EDX-mapping of AuPd/C.

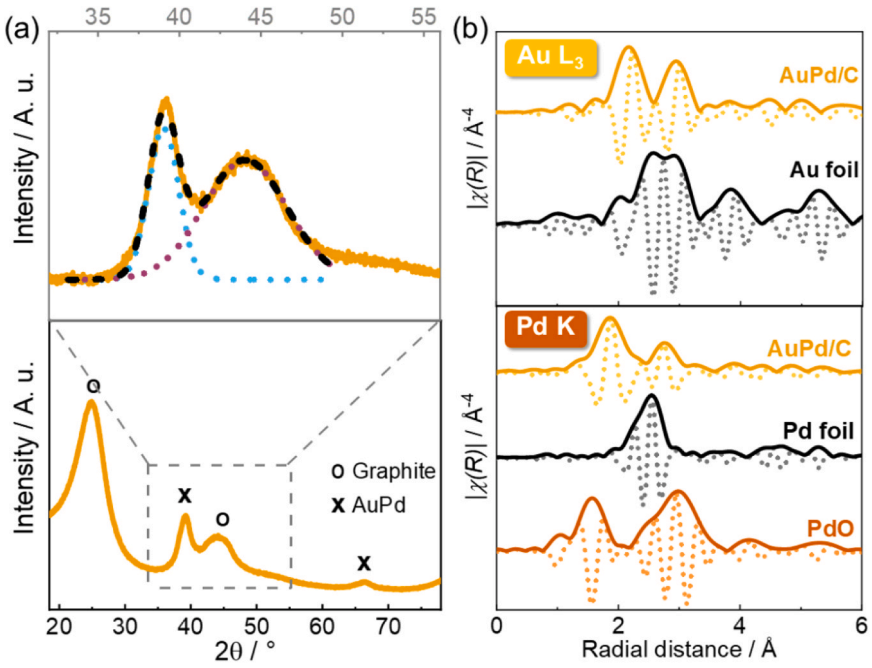

Fig. 2. (a) Powder XRD pattern of AuPd/C (below) and fitting of AuPd and graphite reflection (top). Marking of AuPd reflections according to ICSD reference crystallographic data (Collection code: 58571). (b) Fourier-transformed k^3-weighted EXAFS spectra of AuPd/C measured at Au L_3-edge (top) and Pd K-edge (bottom). Au foil, Pd foil and PdO references are shown.

Table 1
Content of crude, fructose-based HMF solution.

Compound	Concentration / g L^{-1}
HMF	660
Fructose	120
Glucose	10
Levulinic acid	20
Methylglyoxal	10

subsequent deprotection.[46,47]

The crude HMF-solution contained mainly fructose as impurity due to incomplete dehydration, accompanied by other impurities, in particular glucose, levulinic acid, and methylglyoxal, albeit in lower concentrations (<5% compared to HMF, cf. Table 1). Complete conversion of fructose to HMF was deliberately avoided, guided by evidence that fructose can be tolerated by noble metal-based oxidation catalysts.[16] This strategic choice allowed to minimize concentrations of levulinic and formic acid in the solution, which can deactivate the catalytic system.

3.3. Oxidation of crude HMF-solution on AuPd/C under varying reaction conditions

We systematically investigated the selective oxidation of crude HMF-solution using a specially developed AuPd/C catalyst. Employing a 0.1 M HMF-solution as substrate, we studied the influence of varying the base (Na_2CO_3, NaOH) concentration, reaction temperature, and pressure on HMF oxidation (Fig. 3). As reference, we conducted oxidation experiments on a pure HMF-solution (0.1 M, 100 °C, 10 bar air, 5 h, 2 eq. Na_2CO_3, HMF:M 120:1) yielding 100% FDCA at quantitative HMF conversion. In the oxidation of crude HMF-solution, absence of base limited the HMF conversion to 17% (Fig. 3(a)), underscoring the indispensability of base for the reaction. The highest FDCA yields of 94% and 93% were obtained with the addition of 2 and 4 eq. Na_2CO_3, respectively. However, marginal differences were observed among all tested concentrations of added base, resulting in an average FDCA yield of 88%. Hence, we opted for a more sustainable cost-efficient approach by selecting a lower amount of Na_2CO_3 (2 eq.) for the subsequent investigations. While the use of NaOH as base was also tested, its application led to increased HMF degradation, due to the stronger alkalinity, particularly at higher concentrations, limiting further optimization (details, cf. Figure S6). Therefore, we kept Na_2CO_3 as the chosen base for

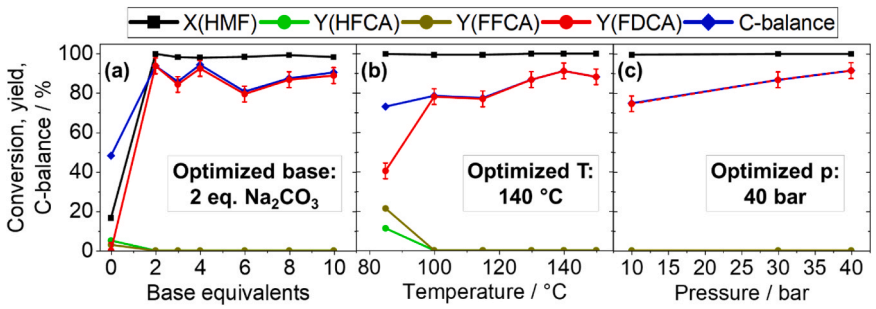

Fig. 3. Influence of (a) Na_2CO_3 equivalents, (b) temperature, and (c) air pressure on the HMF oxidation with AuPd/C (0.1 M HMF, 5 h). (a) 100 °C, 30 bar air, HMF:M 120:1; (b) 30 bar air, 2 eq. Na_2CO_3, HMF:M 230:1; (c) 130 °C, 2 eq. Na_2CO_3, HMF:M 230:1.

the investigation of the influence of other reaction parameters.

We tested HMF:M ratios of 120:1 and 230:1 in the oxidation reaction with 2 eq. Na_2CO_3, resulting in a drop of the FDCA yield from 90% to 78%. For investigating the FDCA yield dependence on temperature and pressure, keeping a lower initial yield helped to accentuate the effect, presenting a more sensitive analysis. In addition, the reduced amount of used catalyst in this scenario confers economic advantage. When varying the reaction temperature, complete HMF conversion was observed over the entire temperature range, with improved FDCA selectivity at higher temperatures (Fig. 3(b)). The highest FDCA yield of 91% was obtained at 140 °C, beyond which a decline in FDCA yield was observed due to HMF and intermediates' degradation. Temperatures below 100 °C hindered the complete conversion of HFCA and FFCA to FDCA. Interestingly, HFCA was not the main side product, which is in contrast to earlier observations of the HMF-oxidation under alkaline conditions. [38] This suggests that the oxidation of the alcohol-function in HFCA does not seem to be the rate-determining step, or other side reactions may be at play at lower temperatures for the crude solution. Thus, the oxidation of the alcohol-function in HFCA to FFCA, and the oxidation of the aldehyde-function in FFCA to FDCA appeared to occur with similar reaction rates, indicated by the FFCA accumulation in the solution. This observation may be attributed to the use of Na_2CO_3 as a base or an influence of the crude solution. Nevertheless, the oxidation of the alcohol function of HMF to DFF was not observed in any experiment of our study.

Finally, the influence of the air pressure on the FDCA yield was monitored (Fig. 3(c)). Air was used as oxidant instead of pure oxygen in all experiments to achieve a greener process owing to its easier handling and cost-effectiveness. We observed an almost linear increase of the FDCA yield with increasing air pressure, reaching a peak of 92% at 40 bar - the highest tested pressure. Employing the optimized reaction conditions (140 °C, 40 bar air, 5 h, 2 eq. Na_2CO_3, HMF:M 230:1) for the oxidation of the crude HMF-solution yielded an impressive FDCA yield of 95% (14.8 g L^{-1}). This corresponds to a remarkable productivity of 34.5 mol_{FDCA} mol_{AuPd}^{-1} h^{-1}.

The reusability of AuPd/C and the stability of its structure after consecutive runs is reported in detail in the supporting information (pages S10 – S11). In brief, AuPd-alloys showed a high stability with no visible phase segregation or oxidation of the noble metals. However, a deactivation was found in the third run, which was ascribed to the blocking of active sites by organic residues.

3.4. Oxidation at higher HMF-concentration by use of a one-pot two-step process with sequential base addition

Upon increasing the HMF concentration beyond 0.1 M, we observed a steady decrease of the FDCA yield under the previously optimized reaction conditions (140 °C, 50 bar air, 5 h, 1 eq. Na_2CO_3, HMF:M 230:1), reaching a minimum of 57% at 0.4 M (cf. Figure S7). To investigate whether the activity loss was due to a lack of active catalytic sites at higher HMF concentrations, we tested different HMF:M ratios at a concentration of 0.3 M (Fig. 4). The FDCA yield dropped from 70% to 52% as the HMF:M ratio increased from 120:1–460:1 (Fig. 4). At the same time, the productivity surged from 25.4 to 75.5 mol_{FDCA} mol_{AuPd}^{-1} h^{-1}. This underlines that the catalyst mass is not the bottleneck for a high FDCA yield when increasing the HMF concentration. However, side reactions, including the degradation of HMF to humins, increased. This occurrence may be due to the higher probability of HMF and hydroxide ions reacting in the liquid phase before reaching the catalyst surface. Nevertheless, the achieved productivity of 75.5 mol_{FDCA} mol_{AuPd}^{-1} h^{-1} exceeded most of the productivities reported for the oxidation of pure HMF-solution, attesting to the remarkable activity of the AuPd-alloy catalysts. [38]

The main challenge in increasing HMF-concentration lies in the higher occurrence of side reactions, causing the HMF degradation to humins. The formation of humins occurs mainly through aldol-condensation reactions involving the aldehyde function of HMF. [48] This happens mostly under elevated temperatures or high alkalinity, as the aldol condensation can be catalyzed by a homogeneous base. [49] Thus, the aldol condensation of HMF under high alkalinity in concentrated solution has to be suppressed. To enable the selective oxidation of HMF in higher concentration, we devised a two-step oxidation process (Scheme 1). In the initial step, we aimed to oxidize HMF predominantly to intermediates, HFCA and FFCA, under mild conditions with the addition of only one eq. Na_2CO_3 to minimize the base quantity. While these conditions may not achieve quantitative oxidation to FDCA, they have the potential to suppress HMF degradation. Subsequently, in the second step, additional base is introduced into the solution, and the temperature is raised to enable the complete oxidation of the intermediates to FDCA under harsher reaction conditions. This split of the HMF oxidation reaction into two steps allows for a streamlined process within the same reactor by simply adding the extra base on the second step. As a result, our approach eliminates the need for additional protection of the aldehyde function with an auxiliary or the draining of the reactor between the steps, rendering it economically more viable.

To limit the amount of varying parameters during the optimization process, we focused on two key parameters for the first step: the reaction temperature and the duration. For the second step, the reaction time and amount of additional base were addressed. The choice of 140 °C for the second step was clued by its ability to give the highest FDCA yield for 0.1 M HMF-concentration, aiming at fast conversion of the intermediates to FDCA. The reaction pressure was 50 bar of synthetic air

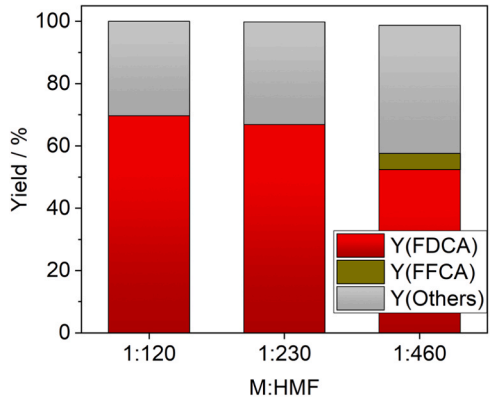

Fig. 4. Oxidation of HMF at different HMF:M ratios (0.3 M HMF, 140 °C, 50 bar air, 5 h, 1 eq. Na_2CO_3).

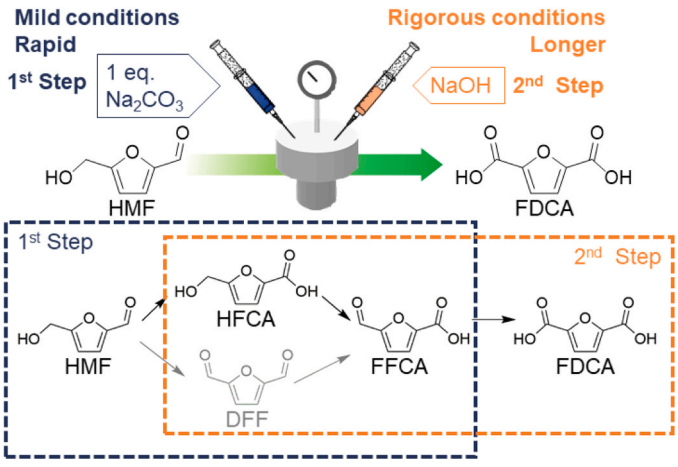

Scheme 1. Schematic representation of a one-pot two-step process for the oxidation of HMF with a first, short reaction step with the addition of 1 eq. Na_2CO_3, and a second, longer reaction step involving the addition of more base.

for both steps, since the catalytic activity was increasing linearly with higher air pressure, which does not influence side reactions.

When investigating the influence of temperature increase during the first reaction step, an increase of the FDCA yield (Fig. 5(a)) was found. However, the C-balance peaked at 100 °C with FFCA being the main oxidation product in the reaction solution. The decrease of the C-balance at higher temperatures can be attributed to HMF degradation at higher temperatures. This effect is more pronounced at HMF-concentration higher than 0.1 M, at which 140 °C was found to be the optimum temperature (Fig. 3). At 70 °C, an incomplete conversion of HMF was observed after 1 h, leading to the identification of 100 °C as the optimal temperature. The C-balance under 80% for all experiments in Fig. 5(a) is ascribed to solubility issues of FDCA and FFCA with only one eq. Na_2CO_3 added to the solution. Hence, a second step with additional 3.3 eq. NaOH to ensure complete dissolution of all compounds was performed with the aim to optimize the reaction time in the first step. The second step was performed at 140 °C and 50 bar air pressure for 4 h while only the time for the first step was varied in Fig. 5(b). The FDCA yield reached a maximum at 1.5 h reaction time in the first step. Longer reaction times led to a decrease in FDCA yield, likely due to the degradation of intermediates in the solution. Consequently, initiating the second reaction step after 1.5 h resulted ideal to sustain an optimal FDCA production.

The first reaction step was subsequently performed at 100 °C and 50 bar air pressure for 1.5 h with the addition of 1 eq. Na_2CO_3. Next, the optimal reaction time for the second step was assessed. In the second reaction step, a FDCA-yield of 77% was obtained after just 1 h (Fig. 5 (c)). A marginal increase of the FDCA-yield was observed with extended reaction time up to a maximum at 4 h. However, no intermediate products were detected in the solution at any reaction time. Therefore, the gradual increase of the FDCA yield over 3 h might be due to a slow dissolution of the remaining FDCA from the surface of the noble metal particles. This underlines the importance of maintaining a sufficient high alkalinity in the solution for the complete dissolution of FDCA when working at elevated concentrations (~ 0.3 M).

Lastly, we investigated the influence of the base in the second reaction step (Fig. 5(d)). The addition of no further base or of four more equivalents Na_2CO_3 in the second step gave low FDCA yields of 65–66%. This indicated that the addition of Na_2CO_3 alone was not sufficient to increase the solubility of FFCA and FDCA, impeding a fast conversion of the intermediates HFCA and FFCA in the second step. The intermediates were partially consumed by degradation. In contrast, adding NaOH in the second reaction step led to a significant increase in FDCA yield with a maximum value of 87% with 3.3 eq. NaOH – the optimal amount for the second step. A further increase of the base amount induced a slight decrease in FDCA yield, due to the formation of undesired side products. Employing these optimized reaction conditions (1st step: 100 °C, 50 bar air, 1.5 h, 1 eq. Na_2CO_3, HMF:M 230:1; 2nd step: 140 °C, 50 bar air, 4 h, 3.3 eq. NaOH), we successfully oxidized a 0.3 M (37.8 g L^{-1}) crude HMF-solution, yielding 87% FDCA (40.7 g L^{-1}) with our specially developed AuPd/C catalyst.

To underline the importance of adding the base in two steps for the oxidation of crude HMF solution at increased concentration (0.3 M), we performed the reaction in one step adding both 1 eq. Na_2CO_3 and 3.3 eq. NaOH, and heating the reaction directly to 140 °C (Fig. 6). The FDCA yield plummeted to a mere 28%. When NaOH was added directly at the

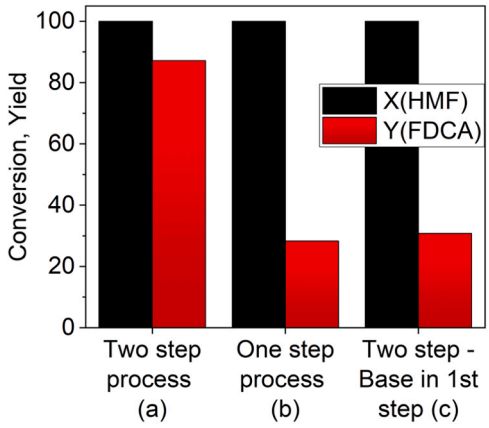

Fig. 6. Comparison of one- and two-step process for the oxidation of crude HMF solution (0.3 M HMF, 50 bar air, HMF:M 230:1). (a): 1st step: 100 °C, 1.5 h, 1 eq. Na_2CO_3; 2nd step: 140 °C, 4 h, 3.3 eq. NaOH. (b): 140 °C, 5.5 h, 3.3 eq. NaOH, 1 eq. Na_2CO_3. (c): 1st step: 100 °C, 1.5 h, 3.3 eq. NaOH, 1 eq. Na_2CO_3; 2nd step: 140 °C, 4 h.

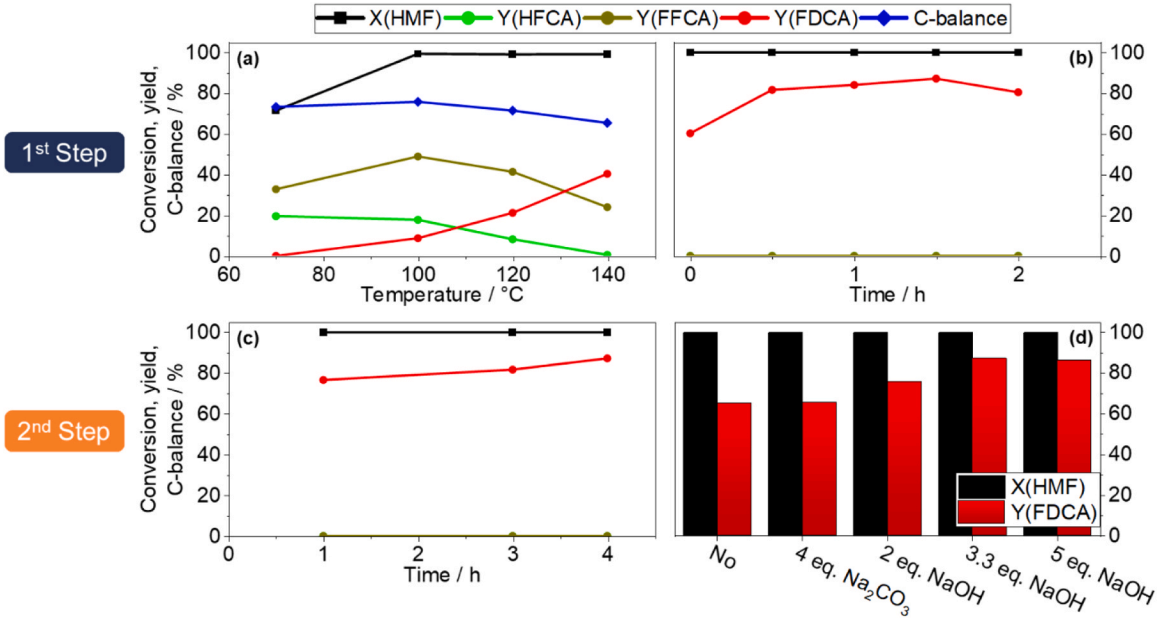

Fig. 5. Influence of (a) temperature, (b+c) time, and (d) base equivalents on the FDCA yield in a one-pot two-step oxidation process of crude HMF solution (0.3 M HMF, 50 bar air, HMF:M 230:1). (a): 1 eq. Na_2CO_3, 1 h; (b): 1st step: 100 °C, 1 eq. Na_2CO_3, 2nd step: 140 °C, 3.3 eq. NaOH, 4 h; (c): 1st step: 100 °C, 1 eq. Na_2CO_3, 1.5 h, 2nd step: 140 °C, 3.3 eq. NaOH; (d): 1st step: 100 °C, 1 eq. Na_2CO_3, 1.5 h, 2nd step: 140 °C, 4 h.

beginning, HMF degradation predominated, leading to humin formation through aldol condensation reactions before oxidation to intermediates could occur. The FDCA yield improved slightly to 31%, if the reaction was kept at 100 °C before increasing the temperature to 140 °C. The temperature of the first step influences the FDCA yield as shown here, however, splitting of the addition of the base appeared to be the most crucial factor for improving the FDCA yield. This "one-pot two-step" approach proved instrumental in accommodating the use of crude HMF solutions with a concentration up to 0.3 M. The achieved FDCA yield of 87% corresponds to a high productivity of 31.6 mol_{FDCA} mol_{AuPd}^{-1} h^{-1}. Remarkably, the AuPd/C catalyst demonstrated robustness against impurities such as fructose, levulinic acid, and humins from the HMF synthesis, even at high concentrations. Despite a slightly lower productivity compared to the diluted 0.1 M HMF-solution, this approach offers economic viability through significant reduction in reaction volume. In addition, it simplifies the product separation by precipitation due to the low solubility of FDCA in water.

A further increase of the HMF-concentration using the crude HMF-solution lead to a decrease of the FDCA yield below 70%. However, refining the reaction conditions, in particular in the first step, to minimize base quantity could effectively suppress the HMF degradation even at elevated concentrations. In addition, employing a lower temperature with an extended reaction time proved advantageous for higher concentrations. This two-step approach was tested with a commercial 1% Au/TiO_2 catalyst (abcr, lot 1368421), but it did not sufficiently convert HMF to FDCA. This emphasizes the necessity for a tailor-made catalyst, enabling a high stability against impurities and high FDCA selectivity from crude solution.

To show the potential of our simplified "one-pot two-step" process for higher HMF-concentrations, and to highlight challenges associated with crude HMF utilization, we performed the selective oxidation of a purified HMF-solution at 0.6 M. Applying almost the same reaction conditions as previously optimized (1st step: 100 °C, 50 bar air, 1.5 h, 1 eq. Na_2CO_3; 2nd step: 140 °C, 50 bar air, 4 h, 1.7 eq. NaOH), we achieved an impressive FDCA yield of 93% with AuPd/C using a 0.6 M HMF-solution. The NaOH-equivalents were reduced to 1.7 eq., since less alkaline conditions can be applied for the oxidation of a purified HMF-solution. In addition, we were able to increase the HMF:M ratio to 290:1. The use of a high HMF:M ratio and an increased HMF-concentration enhances the economic viability of this process by reducing the requirement for expensive noble metals and substantially decreasing of the reactor and solvent volumes. In addition, the absence of extra reaction steps involving the protection and deprotection of HMF with an auxiliary simplifies the process, reducing the complexity, cost, and dead time of the process. Through further optimization of reaction conditions, similar high concentrations might be reached with crude HMF-solutions. Economic simulations of the HMF oxidation process have shown that the HMF price and the cost of the noble metal-based heterogeneous catalyst were key determinants of the final FDCA-price, comprising over 50% of the overall cost.[14] Thus, the direct use of crude HMF-solution, which avoids expensive and complex purification steps following the HMF synthesis, coupled with enhanced concentration and reduced catalyst mass, are significant steps towards lowering the cost of FDCA in a potential heterogeneously catalyzed process.

Nevertheless, several challenges must be addressed to effectively compete with other processes, in particular the homogeneously catalyzed oxidation of HMF to FDCA. Optimization of reaction conditions and base dosing, as demonstrated in our study, is crucial to increase the HMF concentration up to 0.6 M. However, the concentration of HMF in the homogeneous catalytic process is up to about 20 wt%,[18] prompting for further optimization of the heterogeneously catalyzed reaction. The use of concentrated solution is of high importance for decreasing the transportation costs. Moreover, developing an efficient product separation method is essential. Unlike in homogeneous catalysis where FDCA precipitates directly due to the use of acetic acid as solvent, facilitating product separation, preventing catalyst blockage in heterogeneous catalysis requires suppressing precipitation inside the reactor. Thus, the product separation has to be performed afterwards. While literature discusses acidification-induced FDCA precipitation followed by product washing, it is crucial to note that humins, formed particularly from impurities in crude HMF-solution, may also precipitate under such conditions. Therefore, efficient product separation is vital for the future viability of this oxidation route. Finally, further detailed studies on the long-term stability of the catalyst are warranted to justify the investment in noble metal catalysts.

4. Conclusion

Our study demonstrates the applicability of crude, bio-based HMF-solution for the oxidation to FDCA using AuPd-alloys supported on carbon black. Avoiding preliminary purification steps hold the potential to substantially reduce the production costs of FDCA from biomass. Optimizing of oxidation conditions, involving higher temperature (140 °C) and pressure (40 bar), enabled a maximum FDCA yield of 95%. In addition, we developed a "one-pot two-step" process, featuring addition of base in two steps into the same reactor and a transitioning from mild (1st step) to more rigorous conditions (2nd step). This approach allows the utilization of crude HMF-solution with a concentration of 0.3 M. In the initial step, HMF was oxidized under milder conditions - lower temperature (100 °C), less base (1 eq. Na_2CO_3), and under short reaction time (1.5 h) - yielding intermediates HFCA and FFCA, effectively suppressing HMF degradation to humins. In the second step, the intermediates were oxidized to FDCA with an 87% yield under more rigorous conditions - higher temperature (140 °C), more alkaline base (3.3 eq. NaOH), and an extended reaction time (4 h). The threefold concentration increase reduces the reactor volume significantly, which is an important aspect for process up-scaling. Using purified HMF-solution allowed to increase the HMF-concentration up to 0.6 M corresponding to a high HMF:M ratio of 290:1, and a FDCA yield of 93%. Future investigations should explore the transferability of this process, including the split addition of base, into a continuous flow system to enhance overall process efficiency and catalyst utilization. The efficient oxidation of crude HMF-solution produced from abundant agricultural bio-waste to FDCA holds promise to facilitate the up-scaling and industrial implementation of FDCA production.

CRediT authorship contribution statement

Shweta Sharma: Data curation, Formal analysis. **Jan-Dierk Grunwaldt:** Conceptualization, Funding acquisition, Supervision, Writing – review & editing. **Dominik Wüst:** Data curation, Methodology, Writing – review & editing. **Ajai Raj Lakshmi Nilayam:** Data curation, Formal analysis, Writing – review & editing. **Erisa Saraçi:** Conceptualization, Data curation, Project administration, Supervision, Visualization, Writing – review & editing. **Dominik Neukum:** Data curation, Formal analysis, Investigation, Methodology, Writing – original draft.

Declaration of Competing Interest

The authors declare the following financial interests/personal relationships which may be considered as potential competing interests: Erisa Saraci reports financial support was provided by Fachagentur Nachwachsende Rohstoffe eV. If there are other authors, they declare that they have no known competing financial interests or personal relationships that could have appeared to influence the work reported in this paper

Data Availability

Data will be made available on request.

Acknowledgement

The authors would like to thank Veronika Holderied for assistance in HPLC analysis and Armin Lautenbach for ICP-OES analysis. We acknowledge DESY (Hamburg, Germany), a member of the Helmholtz Association HGF, for the provision of synchrotron light. The measurements were performed in the frame of the proposal I-20211473 (DESY) at P65 beamline at PETRA III. We thank Bidyut B. Sarma for help in conducting the respective XAS experiments and data analysis. We would like to thank Edmund Welter for assistance during the beamtimes. STEM imaging was carried out with the support of the Karlsruhe Nano Micro Facility (KNMFi, www.knmf.kit.edu), a Helmholtz Research Infrastructure at Karlsruhe Institute of Technology (KIT, www.kit.edu). This work was financially supported by the Federal Ministry of Food and Agriculture (BMEL) through the FNR (Fachagentur Nachwachsende Rohstoffe e. V.) based on a decision taken by the German Bundestag (funding no. 22010718).

Appendix A. Supporting information

Supplementary data associated with this article can be found in the online version at doi:10.1016/j.cattod.2024.114615.

References

[1] J.H. Clark, Green biorefinery technologies based on waste biomass, Green Chem. 21 (2019) 1168–1170.
[2] J.J. Bozell, G.R. Petersen, Technology development for the production of biobased products from biorefinery carbohydrates—the US Department of Energy's "Top 10" revisited, Green Chem. 12 (2010) 539–554.
[3] R.A. Sheldon, The road to biorenewables: carbohydrates to commodity chemicals, ACS Sustain. Chem. Eng. 6 (2018) 4464–4480.
[4] J.P. Dees, W.J. Sagues, E. Woods, H.M. Goldstein, A.J. Simon, D.L. Sanchez, Leveraging the bioeconomy for carbon drawdown, Green Chem. 25 (2023) 2930–2957.
[5] R.-J. van Putten, J.C. van der Waal, E. de Jong, C.B. Rasrendra, H.J. Heeres, J.G. de Vries, Hydroxymethylfurfural, a versatile platform chemical made from renewable resources, Chem. Rev. 113 (2013) 1499–1597.
[6] A.F. Sousa, C. Vilela, A.C. Fonseca, M. Matos, C.S.R. Freire, G.-J.M. Gruter, J.F. J. Coelho, A.J.D. Silvestre, Biobased polyesters and other polymers from 2,5-furandicarboxylic acid: a tribute to furan excellency, Polym. Chem. 6 (2015) 5961–5983.
[7] E. de Jong, M.A. Dam, L. Sipos, G.J.M. Gruter, Furandicarboxylic Acid (FDCA), A Versatile Building Block for a Very Interesting Class of Polyesters, Biobased Monomers, Polymers, and Materials, American Chemical Society, 2012, pp. 1–13.
[8] M. Sajid, X. Zhao, D. Liu, Production of 2,5-furandicarboxylic acid (FDCA) from 5-hydroxymethylfurfural (HMF): recent progress focusing on the chemical-catalytic routes, Green Chem. 20 (2018) 5427–5453.
[9] P. Pal, S. Saravanamurugan, Recent advances in the development of 5-hydroxymethylfurfural oxidation with base (nonprecious)-metal-containing catalysts, ChemSusChem 12 (2019) 145–163.
[10] D. Zhao, T. Su, Y. Wang, R.S. Varma, C. Len, Recent advances in catalytic oxidation of 5-hydroxymethylfurfural, Mol, Catal 495 (2020) 111133.
[11] S. Hameed, L. Lin, A. Wang, W. Luo, Recent developments in metal-based catalysts for the catalytic aerobic oxidation of 5-hydroxymethyl-furfural to 2, 5-furandicarboxylic acid, Catalysts 10 (2020) 120.
[12] S. Xu, P. Zhou, Z. Zhang, C. Yang, B. Zhang, K. Deng, S. Bottle, H. Zhu, Selective oxidation of 5-hydroxymethylfurfural to 2,5-furandicarboxylic acid using O2 and a photocatalyst of co-thioporphyrazine bonded to g-C3N4, J. Am. Chem. Soc. 139 (2017) 14775–14782.
[13] Z. Zhang, K. Deng, Recent advances in the catalytic synthesis of 2,5-furandicarboxylic acid and its derivatives, ACS Catal. 5 (2015) 6529–6544.
[14] C. Triebl, V. Nikolakis, M. Ierapetritou, Simulation and economic analysis of 5-hydroxymethylfurfural conversion to 2,5-furandicarboxylic acid, Comput. Chem. Eng. 52 (2013) 26–34.
[15] X. Liu, D.C.Y. Leong, Y. Sun, The production of valuable biopolymer precursors from fructose, Green. Chem. 22 (2020) 6531–6539.
[16] W. Naim, O.R. Schade, E. Saraçi, D. Wüst, A. Kruse, J.-D. Grunwaldt, Toward an intensified process of biomass-derived monomers: the influence of 5-(hydroxymethyl)furfural byproducts on the gold-catalyzed synthesis of 2,5-furandicarboxylic acid, CACS Sustain. Chem. Eng. 8 (2020) 11512–11521.
[17] D. Neukum, L. Baumgarten, D. Wüst, B.B. Sarma, E. Saraçi, A. Kruse, J.-D. Grunwaldt, Challenges of Green Production of 2,5-Furandicarboxylic acid from bio-derived 5-hydroxymethylfurfural: overcoming deactivation by concomitant amino acids, ChemSusChem 15 (2022) e202200418.
[18] X. Zuo, P. Venkitasubramanian, K.J. Martin, B. Subramaniam, Facile production of 2,5-furandicarboxylic acid via oxidation of industrially sourced crude 5-hydroxymethylfurfural, ChemSusChem 15 (2022) e202102050.
[19] A. Sanborn, T. Binder, A. Hoffart, Process for making hmf and hmf derivatives from sugars, with recovery of unreacted sugars suitable for direct fermentation to ethanol 2014.
[20] W. Jia, J. Chen, X. Yu, X. Zhao, Y. Feng, M. Zuo, Z. Li, S. Yang, Y. Sun, X. Tang, X. Zeng, L. Lin, Toward an integrated conversion of fructose for two-step production of 2,5-furandicarboxylic acid or furan-2,5-dimethylcarboxylate with air as oxidant, Chem. Eng. J. 450 (2022) 138172.
[21] H. Liu, W. Li, M. Zuo, X. Tang, X. Zeng, Y. Sun, T. Lei, H. Fang, T. Li, L. Lin, Facile and efficient two-step formation of a renewable monomer 2,5-furandicarboxylic acid from carbohydrates over the NiOx catalyst, Ind. Eng. Chem. Res. 59 (2020) 4895–4904.
[22] R.D. Parate, M.S. Dharne, C.V. Rode, Integrated chemo and bio-catalyzed synthesis of 2,5-furandicarboxylic acid from fructose derived 5-hydroxymethylfurfural, Biomass Bioenergy 161 (2022) 106474.
[23] S. Wang, Z. Zhang, B. Liu, Catalytic conversion of fructose and 5-hydroxymethylfurfural into 2,5-furandicarboxylic acid over a recyclable fe3o4–coox magnetite nanocatalyst, ACS Sustain. Chem. Eng. 3 (2015) 406–412.
[24] Z. Yang, W. Qi, R. Su, Z. He, Selective synthesis of 2,5-diformylfuran and 2,5-furandicarboxylic acid from 5-hydroxymethylfurfural and fructose catalyzed by magnetically separable catalysts, Energy Fuels 31 (2017) 533–541.
[25] P.V. Rathod, V.H. Jadhav, Efficient method for synthesis of 2,5-furandicarboxylic acid from 5-hydroxymethylfurfural and fructose using pd/cc catalyst under aqueous conditions, ACS Sustain. Chem. Eng. 6 (2018) 5766–5771.
[26] K. Gupta, R.K. Rai, A.D. Dwivedi, S.K. Singh, Catalytic aerial oxidation of biomass-derived furans to furan carboxylic acids in water over bimetallic nickel–palladium alloy nanoparticles, ChemCatChem 9 (2017) 2760–2767.
[27] P. Scherrer, Bestimmung der Grösse und der inneren Struktur von Kolloidteilchen mittels Röntgenstrahlen, Nachr. Ges. Wiss. Gottingen, Math. -Phys. Kl. 1918 (1918) 98–100.
[28] E. Welter, R. Chernikov, M. Herrmann, R. Nemausat, A beamline for bulk sample x-ray absorption spectroscopy at the high brilliance storage ring PETRA III, AIP Conf. Proc. 2054 (2019).
[29] B. Ravel, M. Newville, Athena, artemis, hephaestus: data analysis for x-ray absorption spectroscopy using IFEFFIT, J. Synchrotron Radiat. 12 (2005) 537–541.
[30] K. Świątek, M.P. Olszewski, A. Kruse, Continuous synthesis of 5-hydroxymethylfurfural from biomass in on-farm biorefinery, Glob. Change Biol. Bioenergy 14 (2022) 681–693.
[31] A. Kruse, K. Swiatek, M. Olszewski, Method and apparatus for purifying a furan derivative, in: U.o. Hohenheim (Ed.), 2022.
[32] L. Vegard, Die Konstitution der Mischkristalle und die Raumfüllung der Atome, Z. F. üR. Phys. 5 (1921) 17–26.
[33] C. Hahn, D.N. Abram, H.A. Hansen, T. Hatsukade, A. Jackson, N.C. Johnson, T. R. Hellstern, K.P. Kuhl, E.R. Cave, J.T. Feaster, T.F. Jaramillo, Synthesis of thin film AuPd alloys and their investigation for electrocatalytic CO2 reduction, J. Mater. Chem. A 3 (2015) 20185–20194.
[34] F. Liu, D. Wechsler, P. Zhang, Alloy-structure-dependent electronic behavior and surface properties of Au–Pd nanoparticles, Chem. Phys. Lett. 461 (2008) 254–259.
[35] G. Tofighi, A. Gaur, D.E. Doronkin, H. Lichtenberg, W. Wang, D. Wang, G. Rinke, A. Ewinger, R. Dittmeyer, J.-D. Grunwaldt, Microfluidic Synthesis of Ultrasmall AuPd Nanoparticles with a Homogeneously Mixed Alloy Structure in Fast Continuous Flow for Catalytic Applications, J. Phys. Chem. C. 122 (2018) 1721–1731.
[36] A.F. Lee, C.J. Baddeley, C. Hardacre, R.M. Ormerod, R.M. Lambert, G. Schmid, H. West, Structural and catalytic properties of novel Au/Pd bimetallic colloid particles: EXAFS, XRD, and acetylene coupling, J. Phys. Chem. 99 (1995) 6096–6102.
[37] O.R. Schade, F. Stein, S. Reichenberger, A. Gaur, E. Saraçi, S. Barcikowski, J.-D. Grunwaldt, Selective aerobic oxidation of 5-(hydroxymethyl)furfural over heterogeneous silver-gold nanoparticle catalysts, Adv. Synth. Catal. 362 (2020) 5681–5696.
[38] O.R. Schade, K.F. Kalz, D. Neukum, W. Kleist, J.-D. Grunwaldt, Supported gold- and silver-based catalysts for the selective aerobic oxidation of 5-(hydroxymethyl) furfural to 2,5-furandicarboxylic acid and 5-hydroxymethyl-2-furancarboxylic acid, Green Chem. 20 (2018) 3530–3541.
[39] E. Taarning, I.S. Nielsen, K. Egeblad, R. Madsen, C.H. Christensen, Chemicals from renewables: aerobic oxidation of furfural and hydroxymethylfurfural over gold catalysts, ChemSusChem 1 (2008) 75–78.
[40] B. Siyo, M. Schneider, J. Radnik, M.-M. Pohl, P. Langer, N. Steinfeldt, Influence of support on the aerobic oxidation of HMF into FDCA over preformed Pd nanoparticle based materials, Appl. Catal., A 478 (2014) 107–116.
[41] H. Ait Rass, N. Essayem, M. Besson, Selective aqueous phase oxidation of 5-hydroxymethylfurfural to 2,5-furandicarboxylic acid over Pt/C catalysts: influence of the base and effect of bismuth promotion, Green. Chem. 15 (2013) 2240–2251.
[42] A. Villa, M. Schiavoni, S. Campisi, G.M. Veith, L. Prati, Pd-modified Au on carbon as an effective and durable catalyst for the direct oxidation of HMF to 2,5-furandicarboxylic acid, ChemSusChem 6 (2013) 609–612.
[43] S.E. Davis, B.N. Zope, R.J. Davis, On the mechanism of selective oxidation of 5-hydroxymethylfurfural to 2,5-furandicarboxylic acid over supported Pt and Au catalysts, Green. Chem. 14 (2012) 143–147.
[44] Z. Liu, Y. Tan, J. Li, X. Li, Y. Xiao, J. Su, X. Chen, B. Qiao, Y. Ding, Ag substituted Au clusters supported on Mg-Al-hydrotalcite for highly efficient base-free aerobic oxidation of 5-hydroxymethylfurfural to 2,5-furandicarboxylic acid, Green Chem. 24 (2022) 8840–8852.
[45] Z. Miao, Y. Zhang, X. Pan, T. Wu, B. Zhang, J. Li, T. Yi, Z. Zhang, X. Yang, Superior catalytic performance of Ce1−xBixO2−δ solid solution and Au/Ce1−xBixO2−δ for

5-hydroxymethylfurfural conversion in alkaline aqueous solution, Catal. Sci. Technol. 5 (2015) 1314–1322.
[46] J.J. Wiesfeld, M. Asakawa, T. Aoshima, A. Fukuoka, E.J.M. Hensen, K. Nakajima, A catalytic strategy for selective production of 5-formylfuran-2-carboxylic acid and furan-2,5-dicarboxylic acid, ChemCatChem 14 (2022) e202200191.
[47] M. Kim, Y. Su, A. Fukuoka, E.J.M. Hensen, K. Nakajima, Aerobic oxidation of 5-(hydroxymethyl)furfural cyclic acetal enables selective furan-2,5-dicarboxylic acid formation with CeO_2-supported gold catalyst, Angew. Chem. Int. Ed. 57 (2018) 8235–8239.
[48] I. vanZandvoort, Y. Wang, C.B. Rasrendra, E.R.H. vanEck, P.C.A. Bruijnincx, H. J. Heeres, B.M. Weckhuysen, Formation, molecular structure, and morphology of humins in biomass conversion: influence of feedstock and processing conditions, ChemSusChem 6 (2013) 1745–1758.
[49] X. Zhang, Y. Li, C. Qian, L. An, W. Wang, X. Li, X. Shao, Z. Li, Research progress of catalysts for aldol condensation of biomass based compounds, RSC Adv. 13 (2023) 9466–9478.